Three-Dimensional Vortex Systems of Finite Wings

Peter Freymuth*
University of Colorado
Boulder, Colorado

Introduction

THE vortex strands of a finite three-dimensional vortex system must be connected in accordance with Helmholtz's law. A piercing question is how well flow visualization documents connecting and reconnecting of the strands. Two-dimensional and other cuts of visualization are incapable of addressing the question. Global visualizations, where we introduce the smoke producing titanium tetrachloride as homogeneously as possible in areas of vorticity production, can document connecting and reconnecting of vortices with moderate success, as our subsequent examples will show.

Global Visualization

Figure 1 shows the top view (global view) of a half-wing protruding from the ceiling into the center of the wind tunnel. It is mounted in a turntable, which allows periodic and other pitchings. The sequence renders global visualization of vortex development in the tip region of the wing. Pitching is ± 5 deg around a 20-deg mean angle of attack; furthermore, $c = 15.2$ cm, $U_0 = 61$cm/s, $f = 0.67$ Hz, and $\Delta t = \frac{1}{8}$ s. Two counterrotating vortices develop near the tip on the suction side of the wing, as columns 1 and 2 show. Both tip vortices join together at the front corner of the tip and, in this way, accommodate the Helmholtz law. The farther inboard vortex also connects to the vortices, which separate from the leading edge. In column 3, both tip vortices move so close together that they may partially annihilate each other by viscous diffusion, thus allowing a growth decay cycle of the tip vortices. Growth and decay of the outer tip vortex has been noticed by Adler and Luttges[1] in their smoke wire visualizations. Vortex tagging thus allowed us to obtain a spanwise or three-dimensional view (global view) of tip vortex development. Furthermore, we have been able to learn how the tip vortices accommodate Helmholtz's law and how a growth-decay cycle can be accommodated.

Figure 2 shows the situation for a pitching delta wing. Periodic pitching is between 0- and 30-deg angles of attack at a reduced frequency $k = 1.6$. In this case, we recognize some growth of the conical leading-edge vortices in column 1. They move toward the centerline of the delta wing. The parts of the tip vortices close to the front corner keep their laminar and straight appearance. Farther downstream they take on somewhat irregular spiral shapes (double spirals, in this case) in the lower frames of column 1. This change in appearance has been observed at constant angle of attack for a long time and is termed "vortex breakdown" or "bursting".[2,3] Near the front corner, the two tip vortices approach each other so closely that they link up and annihilate each other above the link in the upper frames of column 2. The linked-up or reconnected vortex then convects downstream. Simultaneously, new leading-edge vortices start to grow inboard of and close to the leading edges, also in column 2, and go through the entire growth-decay cycle. A growth-decay cycle for a pitching delta wing was first inferred by Gad-el-Hak et al.[4] from their two-dimensional cuts of flow visualization. We now interpret such a cycle by means of three-dimensional vortex principles.

A powerful starting vortex was generated by rapid pitch of a rectangular wing (aspect ratio is 2) from 0- to 60-deg angle of attack within 0.25 s. A photograph of the overall vortex system is shown in Fig. 3. Leading- and trailing-edge vortices are again linked at the front corners of the wing. The main trailing-edge vortex loop is strongly curved toward the back wall of the wind tunnel, which may be visualized by stereoscopic techniques in the future.

Further progress is possible by applying our global visualiation of vortex development to other three-dimensional configurations and pitch time histories.

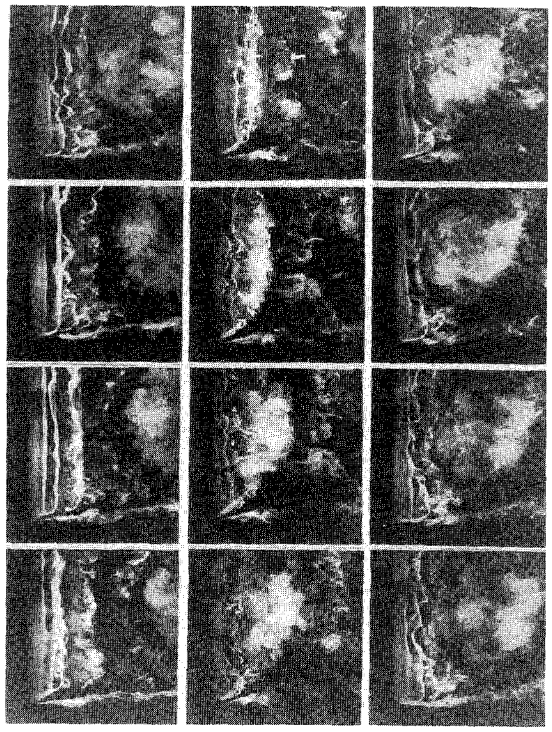

Fig. 1 Rectangular half-wing in periodic pitch around the $c/4$ axis, global or top view, $\alpha = 20$ deg pitch amplitude, $\alpha = 5$ deg, $c = 15.2$ cm, $U_0 = 61$ cm/s, $Re = 5200$, $k = \Pi fc/U_0 = 0.53$, $\Delta t = 1/16$ s.

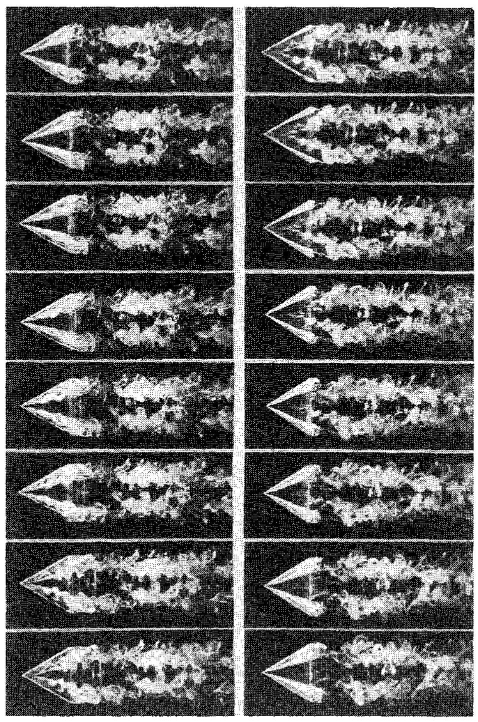

Fig. 2 Equilateral delta wing in periodic pitch around the $c/4$ axis, top view, $\alpha = 15$ deg, $\alpha = 15$ deg, $c = 15.2$ cm = side lengths, $U_0 = 61$ cm/s, $Re = 5200$, $f = 2$ H_z, $k = \Pi fc/U_e = 1.6$, $\Delta t = 1/64$ s.

Received June 25, 1988.

*Professor, Department of Aerospace Engineering Sciences. Member AIAA.

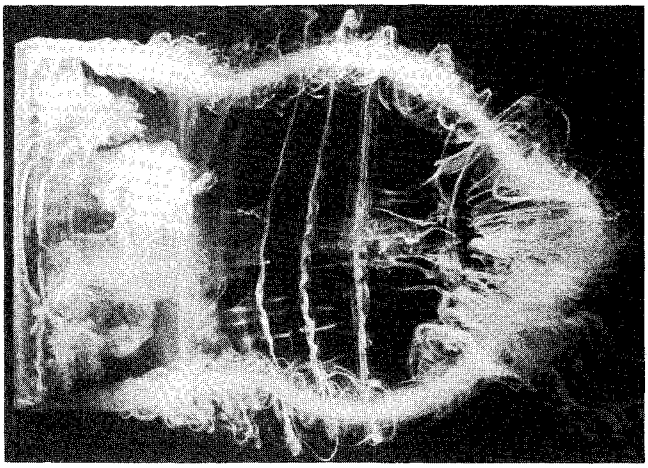

Fig. 3 Top view of vortex system of a rectangular wing with aspect ratio 2 after a rapid pitch from 0 to 60 deg; $c = 15.2$ cm, $U_0 = 61$ cm/s.

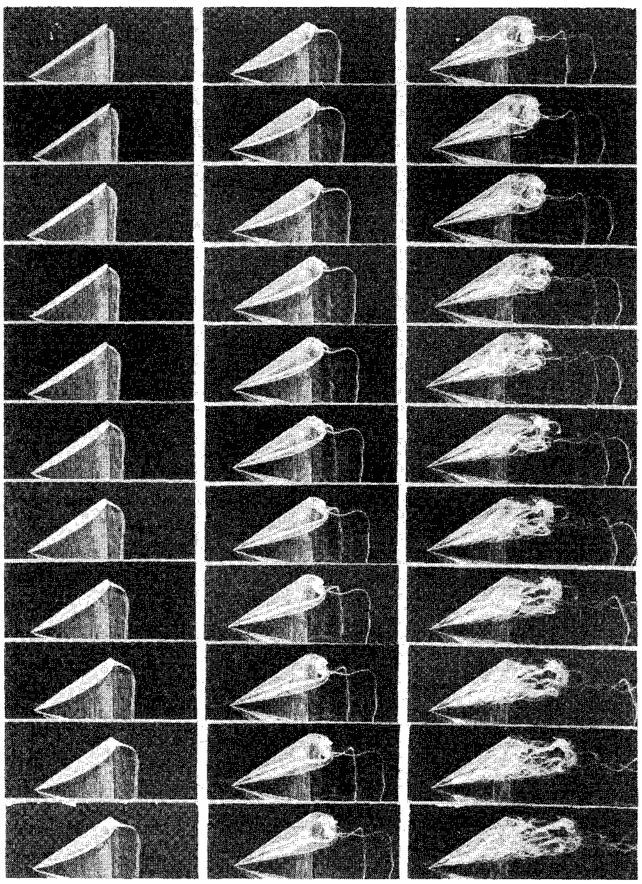

Fig. 4 Close-up top view for a 60-deg delta wing in accelerated starting flow at $\alpha = 40$ deg, $a = 2.4$ m/s^2, $\Delta t = 1/64$ s (15.2 cm wingspan).

Quest for Three-Dimensional Details

Although the previous examples yield good global views of three-dimensional vortex systems, additional vortical detail is desirable in areas where smoke is too dense to visualize the vortical strands fully. To obtain finer detail, we diluted the titanium tetrachloride to 30 vol % by means of trichloroethylene, resulting in less dense smoke production when applied to the wing. We then took close-up movies of areas of interest. An example is shown in Fig. 4, where developments near the upper leading edge of a delta wing at 40-deg angle of attack are shown in a starting flow of constant acceleration. The development of the tip vortex and a trailing-edge starting vortex is shown in column 1. In column 2, a counterrotating secondary vortex develops more closely to the leading edge and connects to the tip vortex near the upper back corner of the wing, as does the trailing-edge vortex and subsequent trailing-edge vortices. In column 3, even this method's efficiency lessens to resolve more fully the various vortex strands that become numerous and turbulent. The last few frames of column 3 show the bursting phenomenon of the main leading-edge tip vortex close to the front corner of the airfoil.

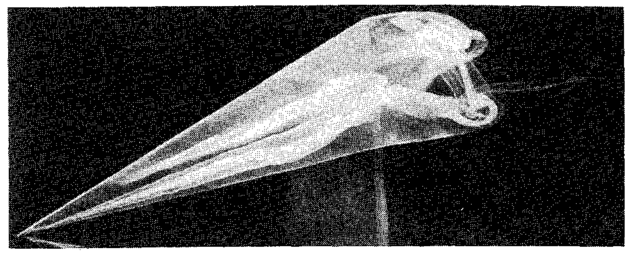

Fig. 5 Enlargement of a photograph corresponding to frame 2, column 3 of Fig. 4.

We previously published a global view of this vortex system,[5,6] which did not produce the fine detail achieved with the dilution method used for Fig. 4. On the other hand, using the dilution method in conjunction with a global view produced inferior overall results.

Figure 5 shows an enlargement of a photograph corresponding to frame 2, column 3 of Fig. 4. This frame shows rather well the linkage knots of the secondary wing vortex and the trailing-edge starting vortex with the leading-edge starting vortex, although all of the details are still not fully resolved. A peculiar vortex bar exists between the two linkage knots.

Our examples show that we are making progress in visualizing the connectivity of vortex strands. Complete resolution is an elusive goal and becomes impossible in a strongly turbulent regime.

Acknowledgments

Air Force Office of Scientific Research Contract F49620-84-C-0065 supported this work. The photographic assistance by W. Bank and F. Finaish is gratefully acknowledged.

References

[1]Adler, J. N. and Luttges, M. W., "Three-Dimensionality in Unsteady Flow About a Wing," AIAA Paper 85-0132, 1985.

[2]Payne, F. M., Ng, T. T., Nelson, R. C., and Schiff, L. B., "Visualization and Flow Survey of the Leading Edge Vortex Structure on Delta Wing Planforms," AIAA Paper 86-0330, 1986.

[3]Lugt, H. J., *Vortex Flow in Nature and Technology,* Wiley, New York, 1983.

[4]Gad-el-Hal, M., Ho, C.-M., and Blackwelder, R. F., "A Visual Study of a Delta Wing in Steady and Unsteady Motion," *Workshop on Unsteady Separated Flow*, U. S. Air Force Academy, Colorado Springs, CO, 1984, pp. 45–51.

[5]Freymuth, P., "Visualizing the Combined System of Wing Tip and Starting Vortices," *TSI Flow Lines*, premier issue, May 1986.

[6]Freymuth, P., Finaish, F., and Bank, W., "Further Visualization of Combined Wing Tip and Starting Vortex Systems," *AIAA Journal*, Vol. 25, 1987, pp. 1153–1159.